Front. Phys., 2014, 9(1): 64–68
DOI 10.1007/s11467-013-0345-5

RESEARCH ARTICLE

Hole arrayed metal-insulator-metal structure for surface enhanced Raman scattering by self-assembling polystyrene spheres

Liang-Ping Xia[1,2], **Zheng Yang**[1,3], **Shao-Yun Yin**[1], **Wen-Rui Guo**[2], **Jing-Lei Du**[3], **Chun-Lei Du**[1,†]

[1] *Chongqing Institute of Green and Intelligent Technology, Chinese Academy of Sciences, Chongqing 401122, China*

[2] *Institute of Optics and Electronics, Chinese Academy of Sciences, P. O. Box 350, Chengdu 610209, China*

[3] *Physics Department, Sichuan University, Chengdu 610064, China*

Corresponding author. E-mail: † *cldu@cigit.ac.cn*

Received March 31, 2013; accepted May 15, 2013

A fabrication process based on the self-assembling polystyrene spheres is proposed to obtain hole arrayed metal-insulator-metal (HA-MIM) structure for surface enhanced Raman scattering (SERS). The localized field enhancement aroused by the gap resonance in the HA-MIM structure is analyzed by finite-different time domain (FDTD) method. With reference to the theory result, the structure is experimentally fabricated and the Raman scattering spectrum of rhodamine 6G (R6G) is measured by a miniaturized Raman spectrometer. The results shows that the enhancement factor is 3.85 times higher than the control sample with single layered metal hole array. The fabrication process to obtain the HA-MIM SERS substrate is reproducible, fast, large area and low cost.

Keywords metal-insulator-metal, surface enhanced Raman scattering, self-assemble, gap resonance

PACS numbers 42.65.Dr, 42.81.Pa, 52.25.Os, 81.07

1 Introduction

Surface plasmons in metallic nanostructures exhibit a strong enhancement of the localized field [1, 2]. With surface plasmon resonance or localized surface plasmon resonance, the Raman scattering from the molecules adsorbed on the metallic nanostructures can be enhanced several orders, which is called Surface-enhanced Raman scattering (SERS) [3]. SERS is a powerful analytical technique in label free and low concentration detection for the fingerprint spectrum and high sensitivity. It has been widely researched in detection of explosive, residual pesticide, contaminative water, medicine, protein and DNA [4–9]. One of the key works in SERS research is how to design and fabricate the substrate with high Raman enhancement factor (EF). It has been demonstrated that the EF is directly related to the localized field intensity [10]. Based on this, kinds of substrates such as metal colloids, rough surface, spheres, and tips [11–15] have been used in SERS. However, the random structures with high EF suffer the limited reproducibility due to the poor reproducible of the hot spots. A probable way to achieve reproducible SERS substrate is to fabricate arrayed structures [16, 17].

Metal-insulator-metal (MIM) arrayed structure is a plasmonic structure which has been widely researched in recent years. Due to the dielectric layer is sandwiched by two metal structure layers, a strong gap resonance can be excited by the coupling of the localized field in the MIM structure. The gap resonance can be easily tuned by changing the metal structure size and the dielectric thickness, hence it has been widely used in perfect absorber, color filter, waveguide and antenna [18–21]. Several papers reported that the MIM structure also performs well in SERS, because the gap resonance positions can be set at the Raman excitation and scattering wavelength synchronously, which can lead to a remarkable enhancement in Raman scattering [22–24]. How to fabricate the MIM structure reliably and fast is the key factor whether it can be widely used in SERS.

In this paper, assembling polystyrene (PS) spheres is proposed to fabricate the SERS substrate with hole arrayed metal-insulator-metal (HA-MIM) structure. The MIM configuration is obtained by coating the metal/SiO_2/metal layers, the hole array is achieved by

etching and then lifting off the PS spheres. The process owns the advantages of assembling PS spheres, which is reproducible, fast, large area and low cost [25]. The gap resonance of the HA-MIM structure is studied firstly by finite-different time domain (FDTD) method. Based on the theory result, the structure is experimentally fabricated and the Raman scattering enhancement of rhodamine 6G (R6G) is measured.

2 FDTD simulation

The simulated HA-MIM structure is shown in Fig. 1(a), based on the process of PS spheres assembling, the hole array is hexagon distributed. The SiO_2 layer in the middle is sandwiched by the gold layers to form the MIM configuration. The distance between the hole center is signed as D and the hole separation is d, the thickness of the SiO_2 layer is t and the thickness of gold layers are fixed to 45 nm. The simulation is carried out by the commercial software Lumerical FDTD Solution and the Palik typed gold is chosen in all of the simulations.

To calculate the gap resonance of the proposed HA-MIM structure, the absorption spectrum is simulated, which is shown in Fig. 1(b). The red curve is for the HA-MIM structure, it shows an absorption peak at the wavelength of 757 nm when $D = 450$ nm, $d = 20$ nm and $t = 20$ nm. However, for the single gold layered structure ($t = 0$ nm), the black curve shows no peak which reveals that the resonance in the HA-MIM structure is excited by the MIM configuration. The electric field distribution at the resonance peak is simulated and shown in the inner figures of Fig. 1(b). The upper one is for the horizontal plane at the center of SiO_2 layer, which shows that the electric field intensity is much stronger in the region of the SiO_2 layer, where the gap resonance occurs. To demonstrate it, the electric field distribution of the vertical plane posited at the red dash line is simulated and shown in the lower figure. The coupling of the top and bottom metal structure makes the gap mode distributed mainly in the region of the SiO_2 layer as analyzed above, which leads to a strong enhancement of the localized field. When the gap resonance mode is located at the wavelength of Raman scattering band, the enhanced localized field will lead to a great enhancement of the Raman scattering.

The relationship of the gap resonance wavelength between the distance of the hole center D is calculated in Fig. 1(c) when $d = 20$ nm, $t = 20$ nm. It shows that the gap resonance wavelength of the HA-MIM structure

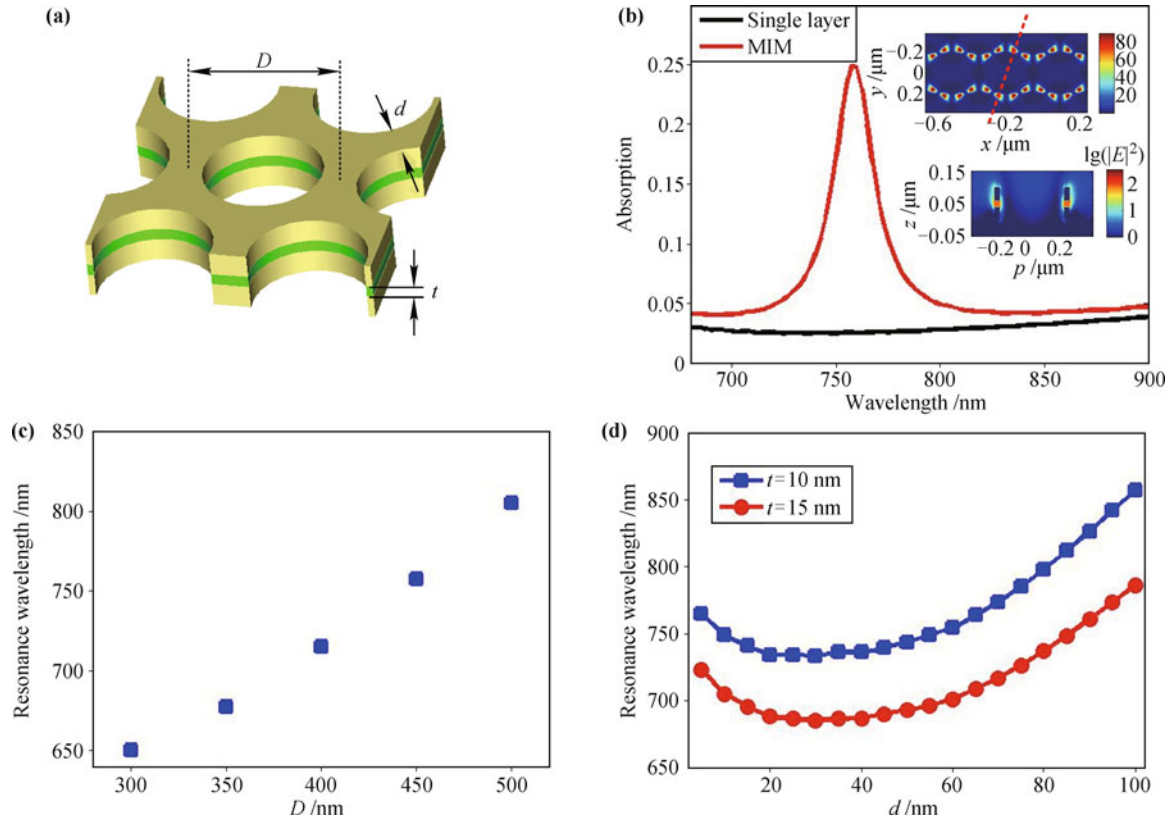

Fig. 1 **(a)** The simulated HA-MIM structure, **(b)** the absorption spectrum and the electric field distribution at the gap resonance wavelength. The relationships of gap resonance wavelength with **(c)** the distance of the hole center D, **(d)** the hole separation d and thickness of the SiO_2 layer t.

is linear increasing with the increasing of D, which fits the surface plasmon resonance theory of grating structure for that D stands for the period of the hole array. Figure 1(d) shows the relationships of the gap resonance wavelength between the hole separation d and the thickness of SiO_2 layer t when $D = 310$ nm. Firstly, the blue curve for $t = 10$ nm is above the red curve for $t = 15$ nm, that is because the increase of the thickness of the dielectric layer in MIM structure leads to the decrease of the wavelength of the gap resonance mode [26]. Secondly, the gap resonance wavelength decreases with the increasing of d when $d < 20$ nm, and then reverse to increases when $d > 40$ nm. In the mid-range of the curves, the gap resonance wavelength is little changed. This behavior can be explained by the Fabry–Perot-type resonator as reported in a previous work [26], which is written as follows:

$$dn_{\text{eff}} = \lambda\eta \tag{1}$$

where n_{eff} is the effective index of the gap resonance mode in the HA-MIM structure, $\eta = (1 - \phi/\pi)/2$, ϕ is the phase acquired by the reflection of the HA-MIM structure at the gap resonance wavelength. This formula shows that d is proportional to the wavelength, hence the gap resonance wavelength increases with the increasing of d when $d > 40$ nm. For the case of $d < 40$ nm, the phase ϕ is not fixed and the proportionality relationship is not existed.

3 Fabrication

The proposed fabrication process of HA-MIM structure is shown in Fig. 2. The first step is self-assembling of PS spheres to obtain a tightly touched periodic structure as shown in Fig. 2(a). Then the reactive ion etching (RIE) is used to etch the PS spheres with oxygen, and the size of the PS spheres become smaller with the distribution remaining the same as shown in Fig. 2(b). In Fig. 2(c), the thin films in the order of gold/SiO_2/gold are coated on the etched PS spheres, when the coating materials transmit through the space between PS spheres, the hole pattern can be formed and deposit on to the substrate. Finally, the HA-MIM SERS structure shown in Fig. 2(d) is obtained by lifting off the PS spheres.

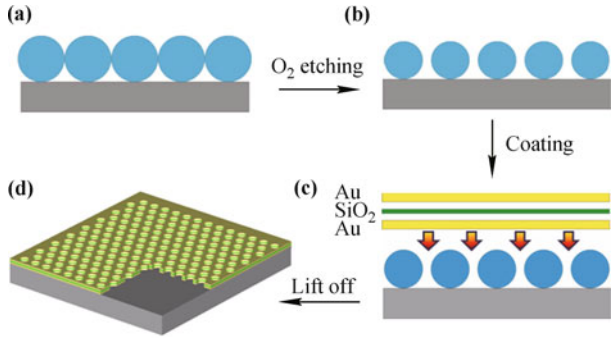

Fig. 2 The schematic of the proposed fabrication process: **(a)** Self-assemble of PS spheres; **(b)** The oxygen etching; **(c)** Gold/SiO_2/gold coating; **(d)** PS spheres lift off and the formed HA-MIM structure.

The process of self-assembling the PS spheres is referenced from a previous work [27]. The PS sphere colloid (from Duke) with the diameter of $D = 310$ nm is used in this step. In the etching process, the RIE power is 45 W, the etching gas is oxygen with the flow of 20 sccm, and the etching time is 150 seconds. The gold layer is coated on with the thickness of 45 nm by thermal evaporation and the SiO_2 layer is coated on by electron beam evaporation with the thickness of 10 nm. The lifting off of the PS spheres is by adhibiting with a flat polydimethylsiloxane (PDMS). In the coating process, the control sample without depositing the SiO_2 layer is fabricated.

With the proposed process, the HA-MIM structure is fabricated and the scanning electron microscope (SEM) pictures are shown in Fig. 3. The first figure is the result of the self-assembled PS spheres, which shows that the spheres are tightly touched. Figure 3(b) is the etched result by RIE, which shows that there are spaces between the spheres. Figure 3(c) is the HA-MIM structure, which shows that the holes are hexagon distributed, and the defects in the structure stem from the self-assembling process.

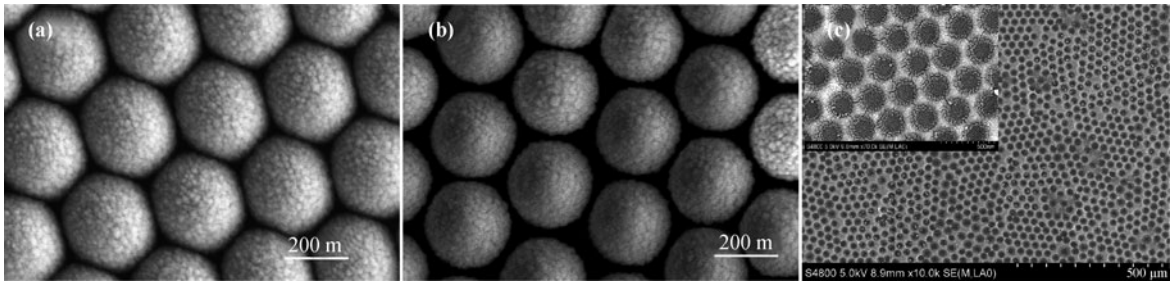

Fig. 3 The SEM figures of the fabrication result: **(a)** The self-assembled PS sphere array; **(b)** The etched result; **(c)** The HA-MIM SERS structure.

4 SERS measurement

The R6G solutions are used to test the Raman enhancement property of the as-prepared HA-MIM SERS substrate. Firstly the R6G (from Sigma-Aldrich, with the purity of 99%) is dissolved in ethanol at the concentration of 1×10^{-2}M and 1×10^{-5}M respectively. Then the Raman spectrums are measured by the miniaturized Raman spectrometer from ocean optics (laser: 785 nm, spectrometer: QE65000). The excitation laser power is 400 mW and the focal spot size on the sample is 300 um with the objective NA=0.22. The Raman spectrum is recorded with the integration time of 5 s. The R6G solution with the concentration of 1×10^{-5}M is dropped on the SERS samples. A reference sample with the concentration of 1×10^{-2}M is dropped on a pure quartz substrate.

The measured Raman spectrum of R6G is shown in Fig. 4, the red curve is for the HA-MIM sample and the green curve is for the control sample with the concentration of 1×10^{-5}M, which shows that the Raman intensity of the HA-MIM structure is much stronger than the control sample. Comparing both of the samples to the quartz substrate with the concentration of 1×10^{-2}M as shown by blue curve, the Raman intensity of the fabricated SERS substrates is largely enhanced. The EF is calculated as follows:

$$EF = \frac{I_{\mathrm{SERS}}}{N_{\mathrm{ads}}} \Big/ \frac{I_{\mathrm{bulk}}}{\mathrm{N}_{\mathrm{bulk}}} \tag{2}$$

where I_{SERS} and I_0 are the intensity of enhanced spectrum and the ordinary spectrum of R6G respectively, N_{ads}, N_{bulk} are the number of R6G molecules adsorbed on SERS substrate and bulk molecules respectively. By this formula, for the three strongest Raman shift at 1317 cm^{-1}, 1369 cm^{-1} and 1520 cm^{-1}, the EF of the HA-MIM structure is 2.8×10^5, 2.88×10^5 and 2.46×10^5 respectively, which is averagely 3.85 times larger than the control sample due to the gap resonance in the HA-MIM structure as analyzed above.

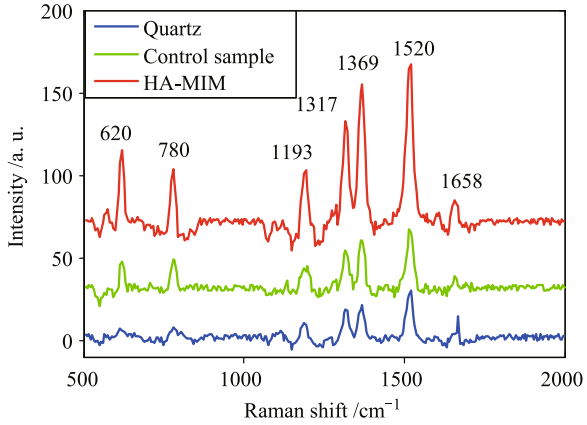

Fig. 4 The Raman spectrum of the R6G with the concentration of 1×10^{-2}M for the quartz and 1×10^{-5}M for the HA-MIM structure and the control sample. The laser wavelength is 785 nm.

5 Conclusion

A process based on the self-assembling of PS spheres to fabricate HA-MIM structured SERS substrate is proposed. The gap resonance and the localized field enhancement are analyzed by FDTD method and the parameter influence is discussed. The HA-MIM structure is fabricated with the proposed process experimentally, which is etching, gold/SiO_2/gold coating and lifting off the PS spheres. The Raman scattering of R6G measurement demonstrates that the gap resonance in the HA-MIM structure leads to the EF 3.85 times larger than the control samples. The proposed process is a candidate to fabricate arrayed SERS substrate with reproducible, fast, large area and low cost.

Acknowledgements This work was supported by Graduate Student Innovation Foundation of Institute of Optics and Electronics, Chinese Academy of Sciences, West Light Foundation of Chinese Academy of Sciences, the National Natural Science Foundation of China (Grant Nos. 11174281 and 61275061), and Funds for Distinguished Young Scientists of Chongqing (Grant No. cstc2012jjjq90001).

References

1. L. Xia, S. Yin, H. Gao, Q. Deng, and C. Du, Sensitivity enhancement for surface plasmon resonance imaging biosensor by utilizing gold-silver bimetallic film configuration, *Plasmonics*, 2011, 6(2): 245
2. C. Li, L. Xia, H. Gao, R. Shi, C. Sun, H. Shi, and C. Du, Broadband absorption enhancement in a-Si:H thin-film solar cells sandwiched by pyramidal nanostructured arrays, *Opt. Express*, 2012, 20(S5): A589
3. A. E. Grow, L. L. Wood, J. L. Claycomb, and P. A. Thompson, New biochip technology for label-free detection of pathogens and their toxins, *J. Microbiol. Methods*, 2003, 53(2): 2213
4. L. Yang, L. Ma, G. Chen, J. Liu, and Z. Tian, Ultrasensitive SERS detection of TNT by imprinting molecular recognition using a new type of stable substrate, *Chemistry*, 2010, 16(42): 12683
5. X. T. Wang, W. S. Shi, G. W. She, L. X. Mu, and S. T. Lee, High-performance surface-enhanced Raman scattering sensors based on Ag nanoparticles-coated Si nanowire arrays for quantitative detection of pesticides, *Appl. Phys. Lett.*, 2010, 96(5): 053104

6. M. Mulvihill, A. Tao, K. Benjauthrit, J. Arnold, and P. Yang, Surface-enhanced Raman spectroscopy for trace arsenic detection in contaminated water, *Angew. Chem.*, 2008, 120(34): 6556
7. A. Campion and P. Kambhampati, Surface-enhanced Raman scattering, *Chem. Soc. Rev.*, 1998, 27(4): 241
8. Hongxing Xu, E. J. Bjerneld, M. Käll, and L. Börjesson, Spectroscopy of single hemoglobin molecules by surface enhanced Raman scattering, *Phys. Rev. Lett.*, 1999, 83(21): 4357
9. K. Kneipp, H. Kneipp, V. B. Kartha, R. Manoharan, G. Deinum, I. Itzkan, R. R. Dasari, and M. S. Feld, Detection and identification of a single DNA base molecule using surface-enhanced Raman scattering (SERS), *Phys. Rev. E*, 1998, 57(6): R6281
10. L. Xia, Z. Yang, S. Yin, W. Guo, S. Li, W. Xie, D. Huang, Q. Deng, H. Shi, H. Cui, and C. Du, Surface enhanced Raman scattering substrate with metallic nanogap array fabricated by etching the assembled polystyrene spheres array, *Opt. Express*, 2013, 21(9): 11349
11. M. T. Sun, Z. L. Zhang, H. R. Zheng, and H. X. Xu, In-situ plasmon-driven chemical reactions revealed by high vacuum tip-enhanced Raman spectroscopy, *Scientific Reports*, 2012, 2: 647
12. M. Sun and H. Xu, A novel application of plasmonics: Plasmon-driven surface-catalyzed reactions, *Small*, 2012, 8(18): 2777
13. Y. Fang, Y. Li, H. Xu, and M. Sun, Ascertaining p, p'-dimercaptoazobenzene produced from p-aminothiophenol by selective catalytic coupling reaction on silver nanoparticles, *Langmuir*, 2010, 26(11): 7737
14. M. Sun, Y. Fang, Z. Zhang, and H. Xu, Activated vibrational modes and Fermi resonance in tip-enhanced Raman spectroscopy, *Phys. Rev. E*, 2013, 87(2): 020401
15. J. Li, Y. Huang, Y. Ding, Z. Yang, S. Li, X. Zhou, F. Fan, W. Zhang, Z. Zhou, D. Wu, B. Ren, Z. Wang, and Z. Tian, Shell-isolated nanoparticle-enhanced Raman spectroscopy, *Nature*, 2010, 464(7287): 392
16. M. Jin, V. Pully, C. Otto, A. Berg, and E. T. Carlen, High-density periodic arrays of self-aligned subwavelength nanopyramids for surface-enhanced Raman spectroscopy, *J. Phys. Chem. C*, 2010, 114(50): 21953
17. K. Li, L. Clime, B. Cui, and T. Veres, Surface enhanced Raman scattering on long-range ordered noble-metal nanocrescent arrays, *Nanotechnology*, 2008, 19(14): 145305
18. L. Xia, H. Gao, H. Shi, X. Dong, and C. Du, A wideband absorption enhancement for P3HT: PCBM addressing by silver nanosphere array, *J. Comput. Theor. Nanosci.*, 2011, 8(1): 27
19. T. Xu, Y. K. Wu, X. G. Luo, and L. J. Guo, Plasmonic nanoresonators for high-resolution colour filtering and spectral imaging, *Nature Communications*, 2010, 1: 59
20. D. Woolf, M. Loncar, and F. Capasso, The forces from coupled surface plasmon polaritons in planar waveguides, *Opt. Express*, 2009, 17(22): 19996
21. B. Y. Choi, D. Choi, and L. P. Lee, Metal-insulator-metal optical nanoantenna with equivalent-circuit analysis, *Adv. Mater.*, 2010, 22(15): 1754
22. Y. Chu, M. G. Banaee, and K. B. Crozier, Double-resonance plasmon substrates for surface-enhanced Raman Scattering with enhancement at excitation and stokes frequencies, *ACS Nano*, 2010, 4(5): 5
23. Y. Chu, D. Wang, W. Q. Zhu, and K. B. Crozier, Double resonance surface enhanced Raman scattering substrates: An intuitive coupled oscillator model, *Opt. Express*, 2011, 19(16): 14919
24. H. C. Kim and X. Cheng, SERS-active substrate based on gap surface plasmon polaritons, *Opt. Express*, 2009, 17(20): 17234
25. B. Z. Wang, W. Zhao, A. Chen, and S.-J. Chua, Formation of nanoimprinting mould through use of nanosphere lithography, *J. Cryst. Growth*, 2006, 288(1): 200
26. M. G. Nielsen, D. K. Gramotnev, A. Pors, O. Albrektsen, and S. I. Bozhevolnyi, Continuous layer gap plasmon resonators, *Opt. Express*, 2011, 19(20): 19310
27. S. Li, S. Yin, Y. Jiang, C. Yin, Q. Deng, and C. Du, Specific protein detection in multiprotein coexisting environment by using LSPR biosensor, *IEEE Transactions on Nanotechnology*, 2010, 9(5): 554